

FIGURE CAPTIONS

Fig. 1. Possible failure modes of an NSM FRP strip: (a) debonding, (b) laminate tensile rupture, (c) concrete semi-conical fracture, (d) mixed shallow semi-cone plus debonding.

Fig. 2. RC beam web: a) axonometric view of the adopted schematization and b) shear loading process.

Fig. 3. Interaction among adjacent strips: a) axonometric view and b) section parallel to the CDC plane.

Fig. 4. NSM shear strength contribution evaluation: flow chart.

Fig. 5. Single Strip Contribution: (a-b) iterative procedure for searching the equilibrium condition in the surrounding concrete; (c) evaluation of the progressive concrete fracture capacity for a single slip in the simple case of orthogonality between strips and CDC and large spacing and (d) in presence of interaction between adjacent strips not orthogonal to the CDC plane.

Fig. 6. Assumed local bond stress-slip relationship: relevant phases of the failure occurring within the adhesive layer.

Fig. 7. Debonding process for an infinite bond length. Distribution of slip, bond stress, strip axial stress and force transferred to the surrounding concrete along the transfer length for the bond phases: (a) elastic, (b) softening and (c) softening friction.

Fig. 8. Free Slipping phase of the debonding process for an infinite bond length: distribution of slip, bond stress, stress in the strip and progressively transferred force.

Fig. 9. Bond wave progressing from the loaded end to the free extremity: (a) invariant distribution of shear stress $\tau(x)$ and slip $\delta(x)$ and the corresponding distribution of strip axial stress $\sigma_f(x)$ and progressive value of the force transferred to the surrounding concrete through bond stresses for an infinite value of the resisting bond length, (b) distribution of slip, tangential stress and progressive force transferred to concrete for a finite value of the resisting bond length and imposed end slip $\delta_{Li}(t_n)$ and for (c) $\delta_{Li}(t_{n+1})$.

Fig. 10. CDC plane: (a) geometrical quantities in OXY and the ellipse local reference system $o_j e_1 e_2 j$; (b) abscissa values necessary to evaluate the i -th ellipse's, both, Linear \mathcal{A}_{fi}^{lin} and Non Linear area \mathcal{A}_{fi}^{nlin} .

Fig. 11. Appraisal of the proposed model for the beams tested by Dias and Barros (2008) and by Dias et al. (2007).

Fig. 12. Cracking scenario regarding beam 2S-7LI45-II: numerical result for $k = 1$ (a), $k = 2$ (b), $k = 3$ (c), and experimental post-test pictures (d-f).

Fig. 13. Comparison between numerical and experimental results: as function of the spacing between adjacent strips at 60° for concrete $f_{cm} 31.1 \text{ MPa}$ (a) and $f_{cm} 18.6 \text{ MPa}$ (b); group effect for the 3rd configuration (concrete $f_{cm} 31.1 \text{ MPa}$ and $\beta 60^\circ$) (c) and ideal shear strength contribution for a system of NSM with spacing 75 mm (d).

Fig. 14. Group effect: (a) a real case with a certain value of the spacing between adjacent strips ($s_{f,real}$), (b) a real case with a reduced value of the spacing ($0.5 \cdot s_{f,real}$) and (c) ideal situation corresponding to the real case depicted in (a).

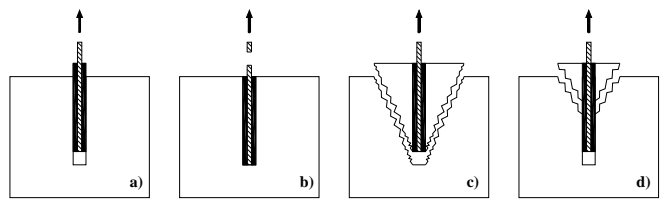


Fig. 1. Possible failure modes of an NSM FRP strip: (a) debonding, (b) laminate tensile rupture, (c) concrete semi-conical fracture, (d) mixed shallow semi-cone plus debonding.

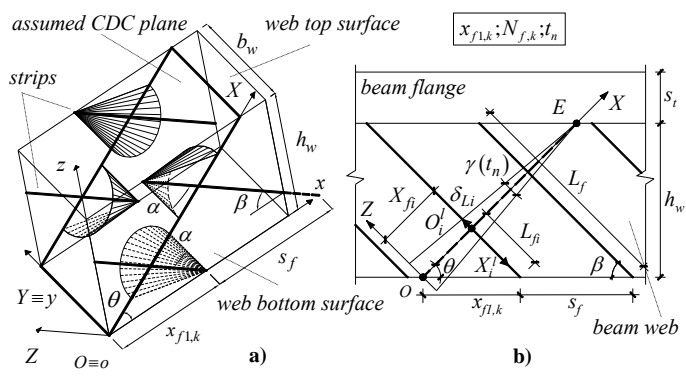


Fig. 2. RC beam web: a) axonometric view of the adopted schematization and b) shear loading process.

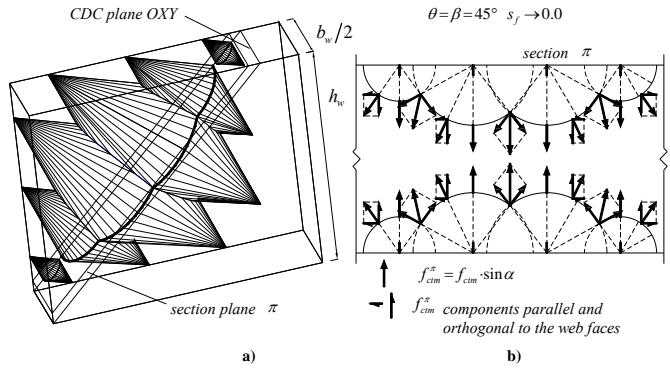


Fig. 3. Interaction among adjacent strips: a) axonometric view and b) section parallel to the CDC plane.

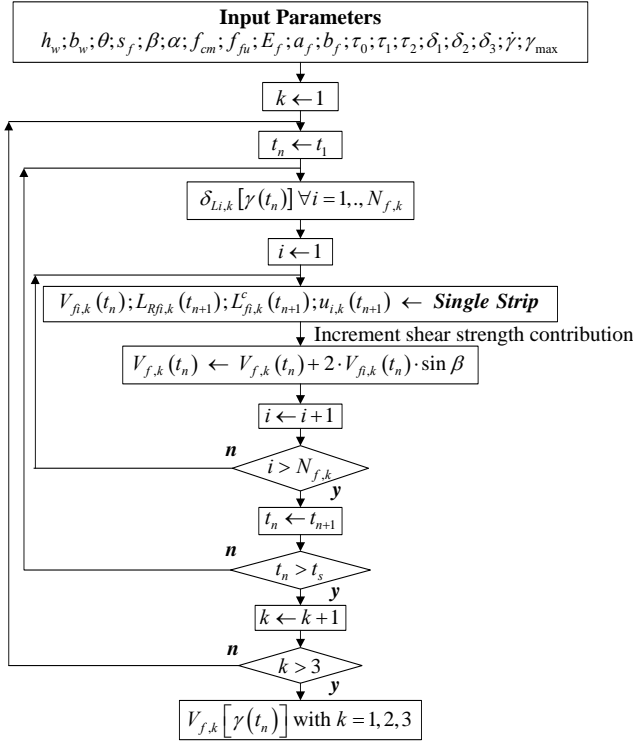


Fig. 4. NSM shear strength contribution evaluation: flow chart.

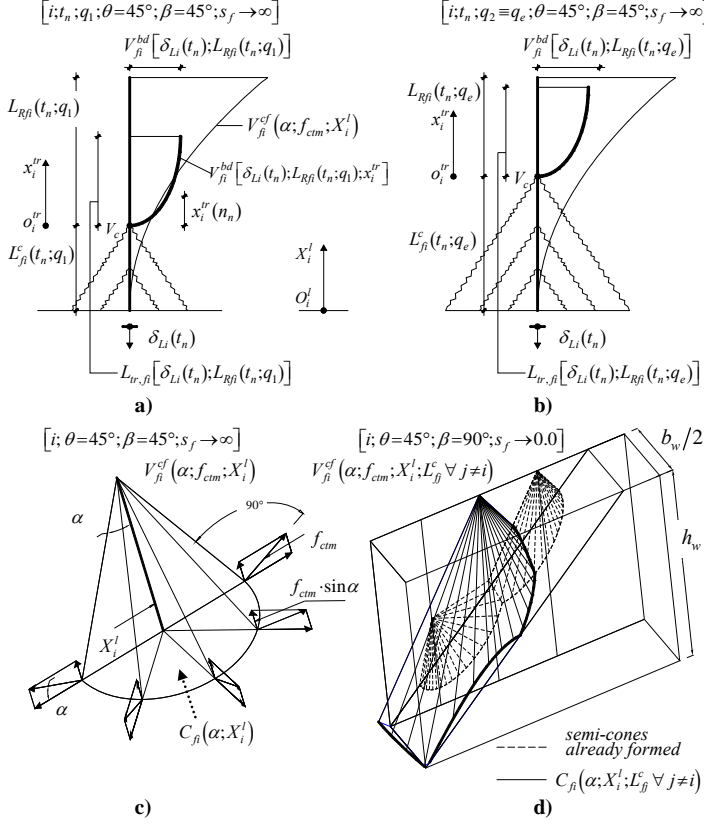


Fig. 5. Single strip contribution: (a-b) iterative procedure for searching the equilibrium condition in the surrounding concrete; (c) evaluation of the progressive concrete fracture capacity for a single strip in the simple case of orthogonality between strips and CDC and large spacing and (d) in presence of interaction between adjacent strips not orthogonal to the CDC plane.

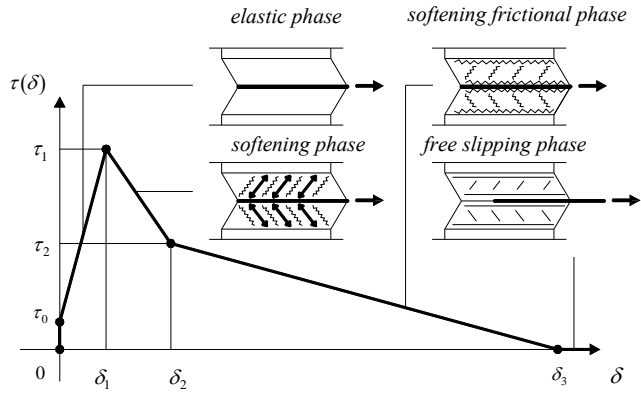


Fig. 6. Assumed local bond stress-slip relationship: relevant phases of the failure occurring within the adhesive layer.

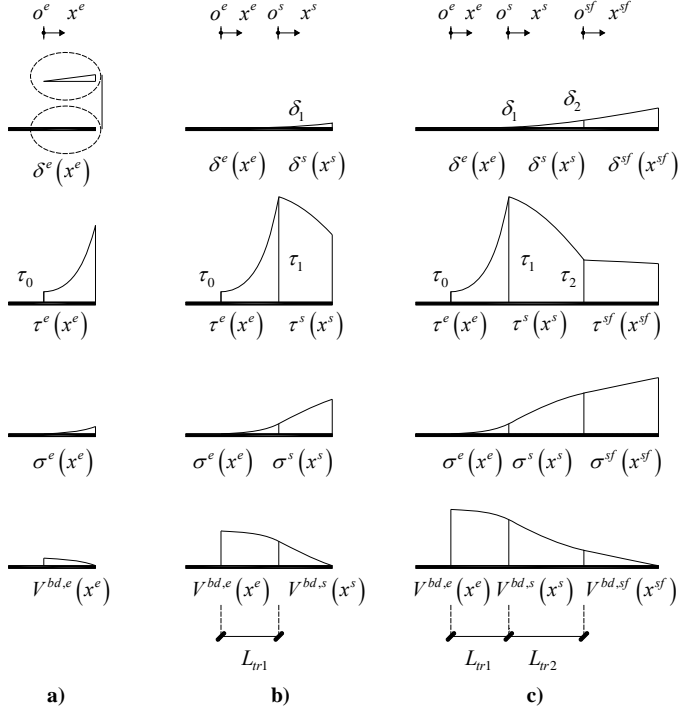


Fig. 7. Debonding process for an infinite bond length. Distribution of slip, bond stress, strip axial stress and force transferred to the surrounding concrete along the transfer length for the bond phases: (a) elastic, (b) softening and (c) softening friction.

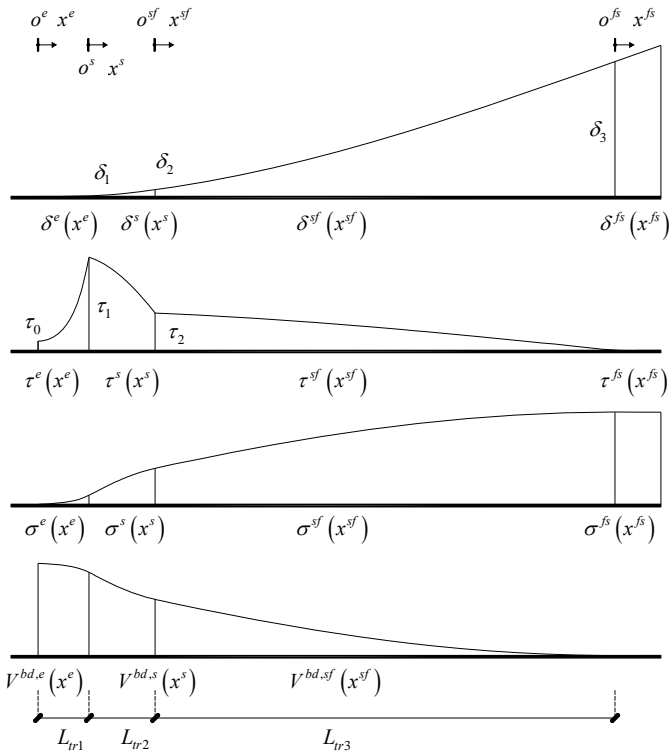


Fig. 8. Free slipping phase of the debonding process for an infinite bond length: distribution of slip, bond stress, axial stress in the strip and progressively transferred force.

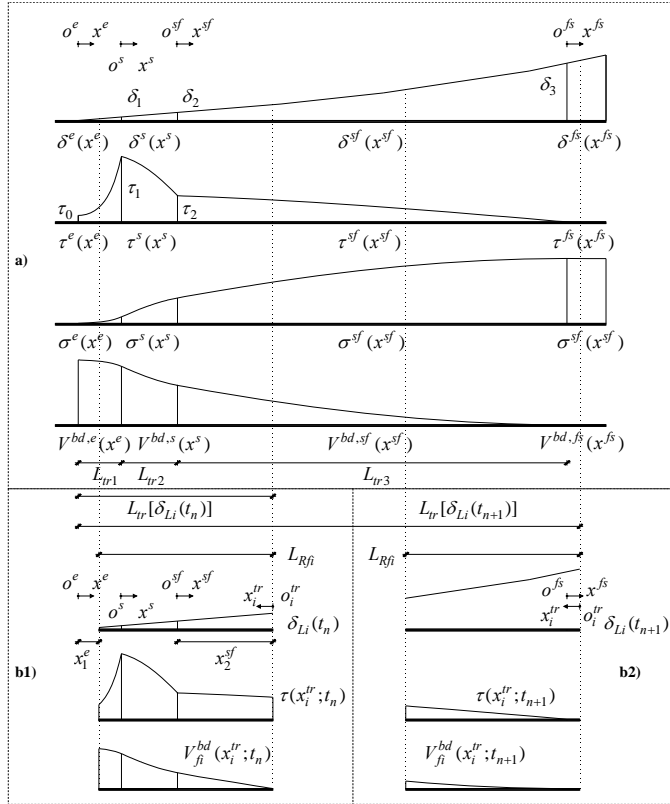


Fig. 9. Bond wave progressing from the loaded end to the free extremity: (a) invariant distribution of shear stress $\tau(x)$ and slip $\delta(x)$ and the corresponding distribution of strip axial stress $\sigma_f(x)$ and progressive value of the force transferred to the surrounding concrete through bond stresses for an infinite value of the resisting bond length, (b) distribution of slip, tangential stress and progressive force transferred to concrete for a finite value of the resisting bond length and imposed end slip $\delta_{Li}(t_n)$ and for (c) $\delta_{Li}(t_{n+1})$.

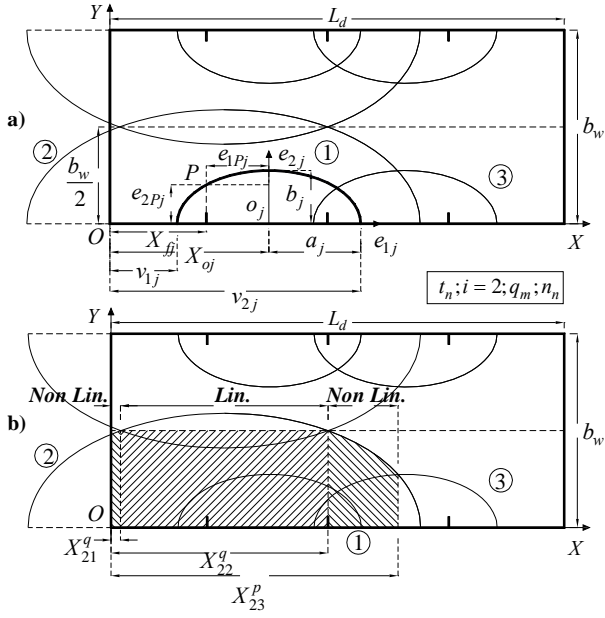


Fig. 10. CDC plane: (a) geometrical quantities in OXY and the ellipse local reference system $o_j e_{1j} e_{2j}$; (b)

abscissa values necessary to evaluate the i -th ellipse's, both, Linear \mathcal{A}_{fi}^{lin} and Non Linear area \mathcal{A}_{fi}^{nlin} .

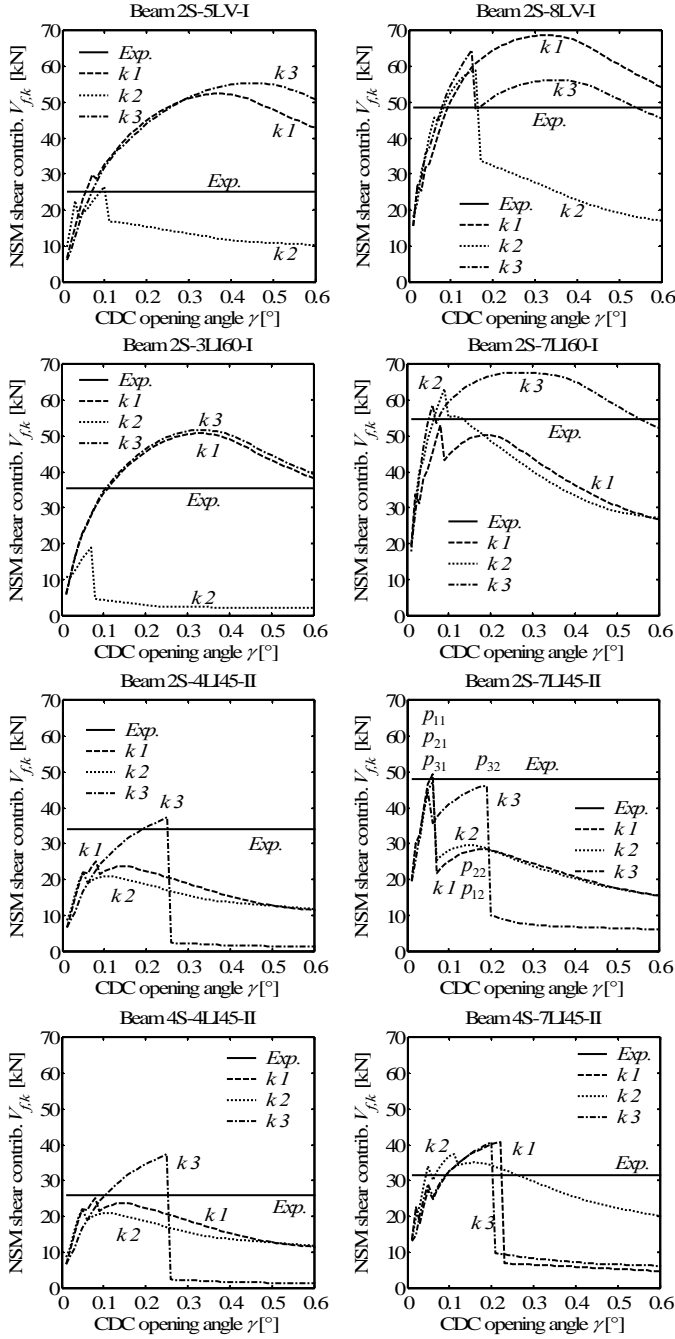


Fig. 11. Appraisal of the proposed model for the beams tested by Dias and Barros (2008) and by Dias et al. (2007).

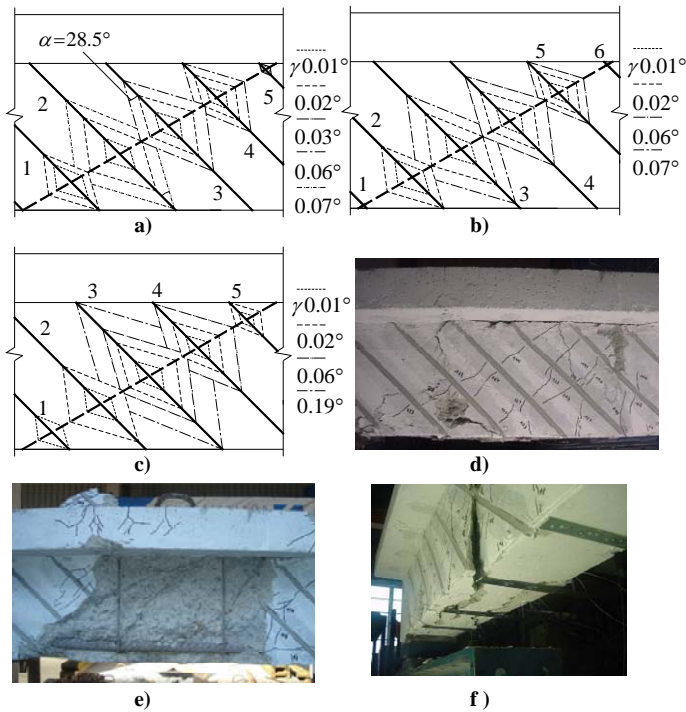


Fig. 12. Cracking scenario regarding beam 2S-7LI45-II: numerical result for $k = 1$ (a), $k = 2$ (b), $k = 3$ (c), and experimental post-test pictures (d-f).

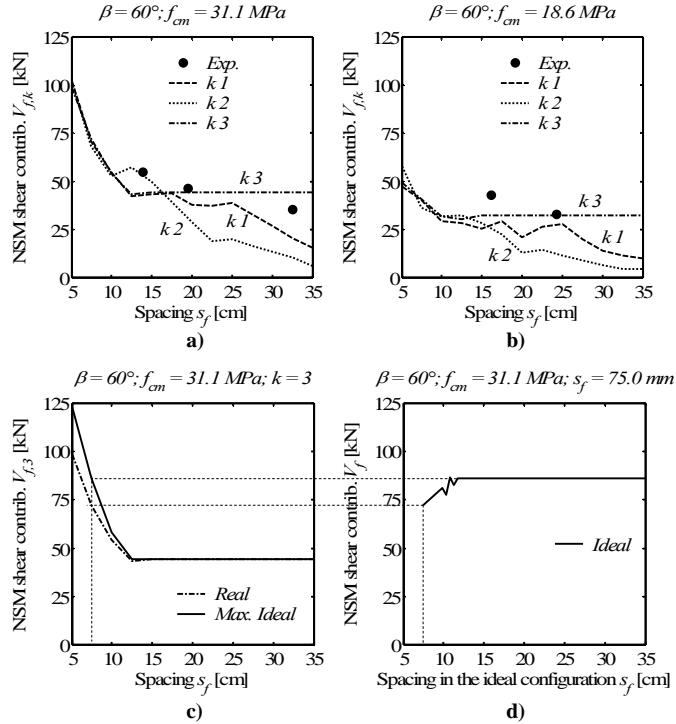


Fig. 13. Comparison between numerical and experimental results: as function of the spacing between adjacent strips at 60° for concrete $f_{cm} 31.1 \text{ MPa}$ (a) and $f_{cm} 18.6 \text{ MPa}$ (b); group effect for the 3rd configuration (concrete $f_{cm} 31.1 \text{ MPa}$ and $\beta 60^\circ$) (c) and ideal shear strength contribution for a system of NSM with spacing 75 mm (d).

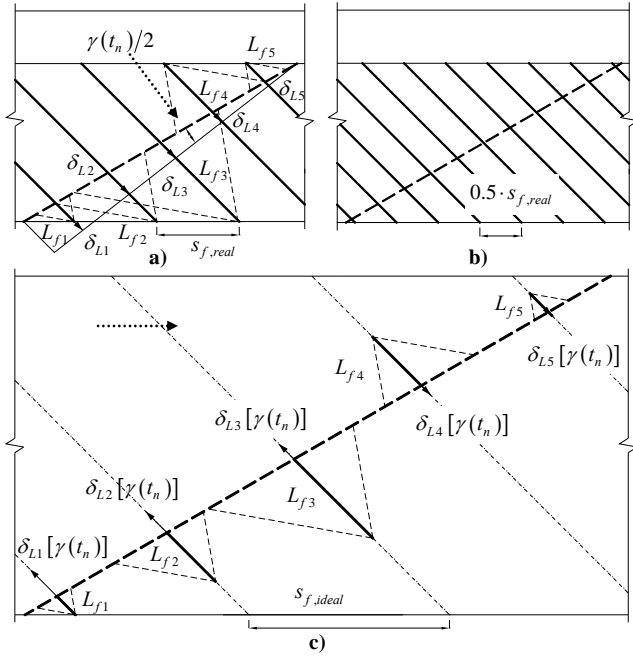


Fig. 14. Group effect: (a) a real case with a certain value of the spacing between adjacent strips ($s_{f,real}$), (b) a real case with a reduced value of the spacing ($0.5 \cdot s_{f,real}$) and (c) ideal situation corresponding to the real case depicted in (a).